Laser Chem., Vol. 14, pp. 119–129
Reprints available directly from the Publisher
Photocopying permitted by license only

OPTICAL–OPTICAL DOUBLE RESONANCE SPECTROSCOPY OF NO_2 IN THE 590.1 NM REGION

KAZUHIKO SHIBUYA, TADASI KUSUMOTO and HIDEKAZU NAGAI

Department of Chemistry, Tokyo Institute of Technology, Ohokayama, Meguro, Tokyo 152, Japan

(Received 24 April 1993)

Optical–optical double resonance (OODR) spectroscopy has been applied to the rotational and vibronic analysis of the thirty nine eigenstates of NO_2 existing in the energy region of 16,980–17,124 cm^{-1} above the ground state. These excited states are concluded to be the mixed states of NO_2 generated by spin–orbit and/or orbital-rotation interaction between the B_2 and A_1 vibronic levels. The mixing mechanism of the excited states is discussed in terms of available information on the visible excited states of NO_2.

KEY WORDS: NO_2, optical-optical double resonance, spin-orbit interaction

1. INTRODUCTION

The visible absorption spectrum of NO_2 is extremely complex and far from the analysis by traditional spectroscopic methods. Its complexity is due to the state interaction of vibronic levels locating at 2–3 eV above the ground state.[1] Even in the supersonic free jet experiments[2–6] where rotation-induced level mixing is minimized, the structure of the origins of the $^2B_2$ vibronic levels is too irregular to be analyzed by a conventional method based on pattern recognition. The number of identified $^2B_2$ vibronic levels exceeds that of vibrational levels of $\tilde{A}^2B_2$ and is nearly equal to that of the high-lying vibrational levels with b_2 symmetry of $\tilde{X}^2A_1$. It is believed that almost all of the a_1 vibrational levels of $\tilde{A}^2B_2$ are vibronically mixed with the high-lying vibrational levels of $\tilde{X}^2A_1$ with b_2 symmetry and make a number of $^2B_2$ vibronic levels responsible for the visible absorption. Brand et al.[7] identified the anomalous transitions in the fluorescence spectra measured by the photoexcitation in the 500 nm region, which was explained by spin–orbit interaction between $\tilde{A}^2B_2$ and the high-lying vibrational levels of $\tilde{X}^2A_1$. Thus, spin–orbit interaction destroys the goodness of rotational quantum numbers, N and K_a in the excited state of NO_2.

An optical–optical double resonance (OODR) method has been applied to the analysis of the visible absorption spectrum of NO_2 and the elucidation of the interaction network of the excited states.[8–13] First, a single rovibronic level in the excited state is prepared as an intermediate state by the first visible laser (ν_1). The second

visible laser (ν_2) excites NO_2 in the intermediate state of interest further to the final state of $2^2B_2(0,0,0)$ locating at 4.98 eV above the ground state. The occurrence of the double resonance was monitored by the ultraviolet emission corresponding to the 2^2B_2–$\tilde{X}^2A_1$ transition. The OODR method offers two major advantages. First, the OODR spectra are simple in rotational structure and easily assigned. The simplification comes from optical selection rules and the state selectivity due to two-photon excitation. Both $^{ev}A_2$–$^{ev}A_1$ and $^{ev}B_1$–$^{ev}B_2$ transitions are optically forbidden under C_{2v} symmetry. Without any state mixing, only $^{ev}B_2$ is expected to be the intermediate state, because the initial and final states are of $^{ev}A_1$ and $^{ev}B_2$ symmetry, respectively. A single rovibronic level can be selected by tuning ν_1 to specific transition energy. Second, the accurate molecular parameters of both the initial and final states are reported[14,15] and hence one can determine the rotational quantum numbers and vibronic symmetry of the intermediate state independently from the ν_1- and ν_2-transitions. Since the symmetry of the final state ($^{ev}B_2$) is different from that of the initial state ($^{ev}A_1$), these types of data have provided information on the state interaction network of NO_2.[9–13]

In this paper, the OODR spectra of NO_2 measured in the 590.1 nm region were analyzed to obtain information on the interaction network in the excitation energy region of 16,980–17,124 cm^{-1}. In many cases, the apparent rotational quantum numbers were assigned to be different depending on the probed transition, ν_1 or ν_2. It is concluded that the intermediate state is a mixed state generated from $^{ev}B_2$ and $^{ev}A_1$ through by spin–orbit interaction with the selection rules, $\Delta N = 0, \pm 1$ and $\Delta K_a = \pm 1$, and/or orbital–rotation interaction with the rules, $\Delta N = 0$ and $\Delta K_a = \pm 1$. The state interaction network of NO_2 is discussed mainly in terms of information based on the OODR experiments.

2. EXPERIMENTAL

The output beam of a XeCl excimer laser (Lambda Physik EMG103E MSC) was split into two beams and used to excite simultaneously two dye lasers (Lambda Physik FL-2002E). The first dye laser was used to excite NO_2 to a rovibronic level in the visible excited state (ν_1-transition). The bandwidth of the ν_1-laser was reduced to 0.04 cm^{-1} by using an intracavity etalon, almost equal to the Doppler width at room temperature. The second dye laser (the bandwidth of 0.3 cm^{-1}) was used to excite NO_2 in the intermediate state further to the 2^2B_2 state (ν_2-transition). The delay time of about 20 ns between the two laser pulses was set to avoid the first step absorption by the ν_2-laser. Dyes used were LC-5900 and LC-4200 (Lambda Physik). The wavenumber calibrations of ν_1 and ν_2 were made by measuring the LIF excitation spectrum of iodine (the estimated precision of 0.04 cm^{-1}) and the opto-galvanic spectrum of Ne (the estimated precision of 0.3 cm^{-1}), respectively. The UV fluorescence was detected by a solar-blind photomultiplier (Hamamatsu R166) after being passed through a bandpass filter (Corning 7-54). The signals were amplified by a preamplifier (PAR 105, x10) and averaged with a boxcar integrator (PAR 162/165). The NO_2 pressure was kept constant at 1.0 Torr throughout the experiments.

3. RESULTS

Figure 1 shows typical two kinds of OODR spectra measured in this OODR experiment. The ν_2-scanned spectrum (a) was measured by fixing ν_1 at 16,939.09 cm^{-1} and scanning ν_2 over 23,140–23,190 cm^{-1}. Under C_{2V} symmetry, the B_2–B_2 transition is of a perpendicular type with the optical selection rules, $\Delta N = 0, \pm 1$ and $\Delta K_a = \pm 1$. As shown in Figure 1a, the ν_2-scanned OODR spectrum typically consists of six lines, exhibiting the rotational structure of $2^2B_2(0,0,0)$. The terminating rotational level in the 2^2B_2 state could be easily assigned as indicated in Figure 1a, using the molecular parameters reported for the final state of $2^2B_2(0,0,0)$.[15] Taking account of

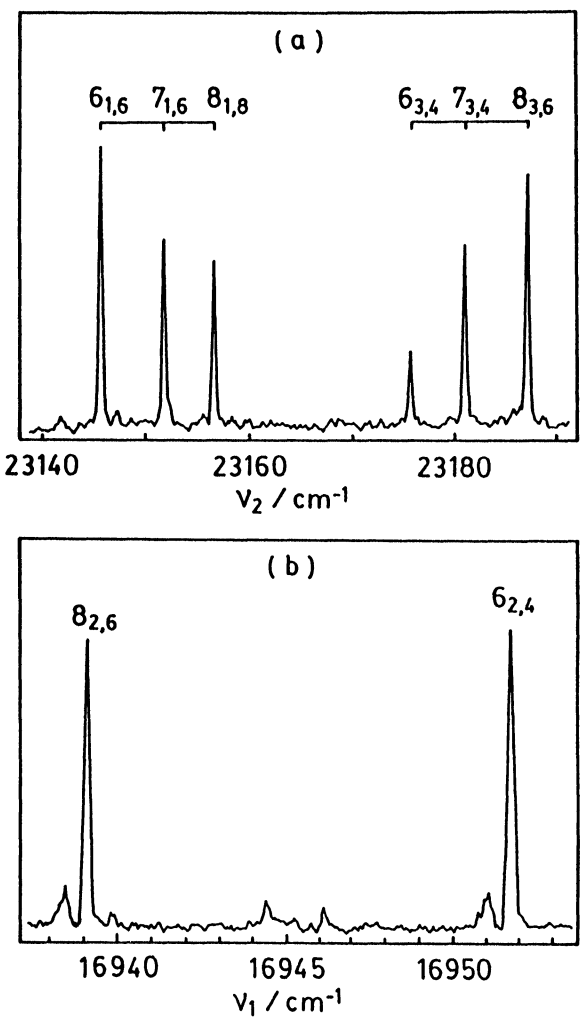

Figure 1 (a) A ν_2-scanned OODR spectrum measured by fixing ν_1 at 16,939.09 cm^{-1}. (b) A ν_1-scanned OODR spectrum measured by fixing ν_2 at 23,145.4 cm^{-1}.

the assignments and the selection rules on the transition, the rotational quantum number of the intermediate level could be assigned to $7_{2,5}$.

Figure 1b shows the ν_1-scanned OODR spectrum obtained by fixing ν_2 at 23,145.4 cm^{-1}, $^pP_2(7)$ in the spectrum shown in Figure 1a. Exactly the same OODR spectrum was obtained when the ν_2-wavenumber was tuned to any of the other five lines measured in Figure 1a. In the ν_1-scanned OODR spectrum, the ν_2-wavenumber was fixed at certain transition energy terminating on a single rovibronic level of $2^2B_2(0,0,0)$. Then, the OODR spectrum observed corresponds to the excitation spectrum from the ground $\tilde{X}^2A_1$ state to a specified rotational level in the intermediate vibronic state. The A_1–B_2 transition is of a parallel type, with the optical selection rules, $\Delta N = 0, \pm 1$ and $\Delta K_a = 0$. Line strength of ^qQ branch ($\Delta N = \Delta K_a = 0$) is so weak that most of the ^qQ branches could not be observed in this experiment. As a result, the ν_1-scanned OODR spectrum consists of two lines, ^qP and ^qR, as shown in Figure 1b. The originating rotational levels in the $\tilde{X}^2A_1$ state responsible for the two lines can be easily assigned as indicated in Figure 1b, using the molecular parameters reported for the initial state, $\tilde{X}^2A_1(0,0,0)$.[14] Thus, the rotational quantum number of the intermediate vibronic state, $N'_{Ka,Kc}$ (ν_1), was assigned to $7_{2,5}$.

The assignment procedures mentioned above were used to obtain the rotational quantum number of the intermediate state. As a result, the quantum numbers and vibronic symmetry of the intermediate state were determined independently from the ν_1- and ν_2-scanned spectra. To avoid confusion, the rotational quantum numbers of the intermediate state are denoted by $N'_{Ka,Kc}(\nu_1)$ and $N'_{Ka,Kc}(\nu_2)$ corresponding to the probed ν_1- and ν_2-transitions, respectively. In the case of the intermediate state shown in Figure 1, the numbers of $N'_{Ka,Kc}(\nu_1)$ accord with those of $N'_{Ka,Kc}(\nu_2)$: $N'_{Ka,Kc}(\nu_1) = N'_{Ka,Kc}(\nu_2) = 7_{2,5}$. The total excitation energy of E_{evr}, which is the sum of electronic, vibrational and rotational energies, is determined to be 16,999.82 cm^{-1}. In the same manner, many OODR spectra were measured and analyzed in the ν_1-region of 16,930–16,980 cm^{-1}. The results are listed in Table I. The bandwidth of the ν_1-laser was comparable with the spin splittings. In some cases, the F_1 and F_2 levels could be assigned from the sum of ν_1- and ν_2-wavenumbers. On the basis that the total angular momentum J must be conserved in the isolated molecule, it was possible to determine whether the intermediate rovibronic level belongs to F_1 or F_2. One can recognize many levels of $N'(\nu_2)$ different from $N'(\nu_2)$, which indicates that the intermediate levels are generated from at least two vibronic states through some coupling forces.

4. DISCUSSION

4.1. Detection of mixed states in the 590.1 nm region

Among thirty nine intermediate levels listed in Table I, twenty four levels have the quantum numbers of $N'(\nu_2)$ identical with those of $N'(\nu_1)$, while fifteen levels have the $N'(\nu_2)$ numbers different from $N'(\nu_1)$. All the thirty nine rovibronic levels have

Table I OODR transitions and assignments measured in the 590.1 nm region

E_{evr} (cm^{-1})	*Assignment*	ν_1 (cm^{-1})	$N'_{Ka,Kc}(\nu_1)$	$N'_{Ka,Kc}(\nu_2)$	$\Delta N'$
16979.89	Q(2)	16947.28	$2_{2,1}F_2$	$2_{2,1}F_2$	0
	P(3)	16944.64			
16979.97	R(3)	16944.74	$4_{2,3}F_2$	$3_{2,1}F_1$	–1
	P(5)	16937.08			
16981.46	R(2)	16948.52	$3_{2,1}F_2$	$2_{2,1}F_1$	–1
	Q(3)	16946.24			
	P(4)	16942.80			
16983.00	R(2)	16950.09	$3_{2,1}F_1$	$3_{2,1}F_1$	0
	P(4)	16944.21			
16984.81	R(3)	16949.59	$4_{2,3}F_2$	$3_{2,1}F_1$	–1
	P(5)	16941.92			
16985.67	R(2)	16952.76	$3_{2,1}F_1$	$4_{2,3}F_2$	+1
	P(4)	16946.87			
16986.31	R(3)	16950.89	$4_{2,3}F_1$	$4_{2,3}F_1$	0
	P(5)	16943.32			
16988.64	R(4)	16949.98	$5_{2,3}$	$5_{2,3}$	0
	P(6)	16940.70			
16988.81	R(5)	16945.93	$6_{2,5}F_2$	$5_{2,3}F_1$	–1
	P(7)	16934.94			
16989.69	R(3)	16954.25	$4_{2,3}F_1$	$5_{2,3}F_2$	+1
	P(5)	16946.70			
16989.70	R(4)	16951.06	$5_{2,3}F_2$	$5_{2,3}F_2$	0
	P(6)	16941.74			
16990.85	R(4)	16952.06	$5_{2,3}F_1$	$5_{2,3}F_1$	0
	P(6)	16942.80			
16993.94	R(5)	16951.09	$6_{2,5}F_2$	$6_{2,5}F_2$	0
	P(7)	16940.05			
16994.21	R(6)	16946.25	$7_{2,5}F_2$	$6_{2,5}F_1$	–1
	P(8)	16933.56			
16994.42	R(4)	16955.65	$5_{2,3}F_1$	$6_{2,5}F_2$	+1
	P(6)	16946.35			
16995.04	R(5)	16952.06	$6_{2,5}F_1$	$6_{2,5}F_1$	0
	P(7)	16941.08			
16995.85	R(5)	16952.85	$6_{2,5}F_1$	$6_{2,5}F_1$	0
	P(7)	16941.91			
16999.53	R(6)	16951.57	$7_{2,5}F_2$	$7_{2,5}F_2$	0
	P(8)	16938.89			
16999.82	R(6)	16951.78	$7_{2,5}F_1$	$7_{2,5}F_1$	0
	P(8)	16939.09			

Table I (*cont'd*)

E_{evr} (cm^{-1})	*Assignment*	ν_1 (cm^{-1})	$N'_{Ka,Kc}(\nu_1)$	$N'_{Ka,Kc}(\nu_2)$	$\Delta N'$
17000.11	R(7) P(9)	16946.26 16931.85	$8_{2,7}F_2$	$7_{2,5}F_1$	−1
17001.22	R(6) P(8)	16953.18 16940.55	$7_{2,5}$	$7_{2,5}$	0
17001.98	R(6) P(8)	16954.03 16941.31	$7_{2,5}F_2$	$7_{2,5}F_2$	0
17002.45	R(7) P(9)	16948.58 16934.21	$8_{2,7}F_2$	$7_{2,5}F_1$	−1
17007.35	R(8) P(10)	16946.70 16930.64	$9_{2,7}F_2$	$8_{2,7}F_1$	−1
17007.46	R(7) P(9)	16953.56 16939.24	$8_{2,7}$	$8_{2,7}$	0
17007.72	R(7) P(9)	16953.78 16939.41	$8_{2,7}F_1$	$9_{2,7}F_2$	+1
17008.90	R(7) P(9)	16954.95 16940.61	$8_{2,7}$	$8_{2,7}$	0
17014.32	R(8) P(10)	16953.66 16937.62	$9_{2,7}$	$9_{2,7}$	0
17014.90	R(8) P(10)	16954.19 16938.14	$9_{2,7}$	$9_{2,7}$	0
17023.49	R(9) P(11)	16955.25 16937.52	$10_{2,9}$	$10_{2,9}$	0
17024.36	R(9) P(11)	16956.14 16938.36	$10_{2,9}$	$10_{2,9}$	0
17032.09	R(10) P(12)	16955.38 16935.94	$11_{2,9}$	$11_{2,9}$	0
17033.68	R(10) P(12)	16956.98 16937.51	$11_{2,9}F_2$	$10_{2,9}F_1$	−1
17066.36	R(13) P(15)	16959.29 16934.79	$14_{2,13}$	$14_{2,13}$	0
17066.86	R(13) P(15)	16959.73 16935.33	$14_{2,13}$	$14_{2,13}$	0
17068.15	R(12) Q(13) P(14)	16971.95 16961.06 16949.14	$13_{2,11}F_1$	$14_{2,13}F_2$	+1
17094.69	R(15) P(17)	16963.14 16935.30	$16_{2,15}$	$16_{2,15}$	0
17104.40	R(16) P(18)	16959.19 16929.56	$17_{2,15}$	$17_{2,15}$	0
17124.05	R(16) P(18)	16978.82 16949.21	$17_{2,15}F_1$	$18_{2,17}F_2$	+1

an identical K_a number; $K_a'(\nu_1) = K_a'(\nu_2) = 2$. There are three types of the relations between $N'(\nu_1)$ and $N'(\nu_2)$: $\Delta N' = N'(\nu_2) - N'(\nu_1) = 0$ and ± 1. Figures 2 and 3 plot the energies of all the intermediate levels listed in Table I against the rotational quantum numbers $N'(\nu_2)$ and $N'(\nu_1)$, respectively. If NO_2 is a regular molecule, the reduced level energies, $E_{red} = E_{evr} - 0.3N'(N' + 1)$, should have a linear correlation vs. $N'(N' + 1)$.

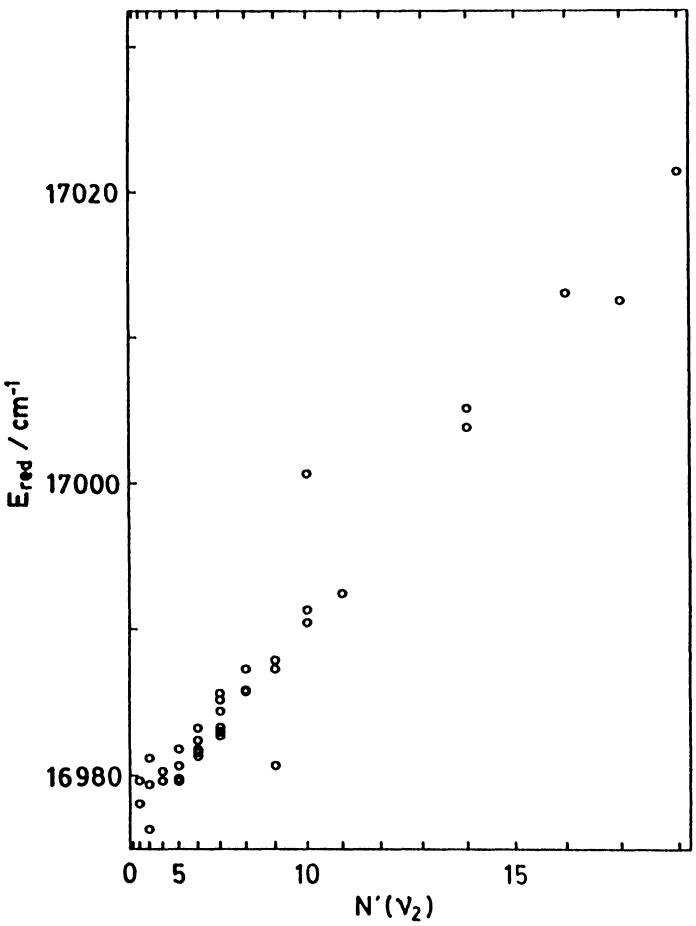

Figure 2 Plot of the reduced rovibronic energies, $E_{red} = E_{evr} - 0.3N'(N' + 1)$, against $N'(N' + 1)$. Here, N' denotes $N'(\nu_2)$. Fitting of the data to the equation, $E_{evr} = T_v + (A–\bar{B})K_a^2 + \bar{B}N(N + 1)$, gives the molecular constants; $T_v \sim 16{,}947$ cm^{-1} and $\bar{B} \sim 0.43$ cm^{-1} assuming that $(A–\bar{B}) = 7.5$ cm^{-1}.

Roughly speaking, the E_{evr} vs. $N'(\nu_2)$ plot exhibits a linear relation as shown in Figure 2. Many levels with the same N' and K_a' quantum number exist in the energy region spread over a few wavenumbers. There exist six levels with an identical rotational quantum number of $N'(\nu_2) = 7$. Five levels exist as $N'(\nu_2) = 5$ or 6, and

three levels as $N'(\nu_2)$ = 3, 8, 9, or 10. The maximum number of levels with an identical rotational N′ and K′ quantum number was six in the 590.1 nm region. If NO_2 is a regular molecule, the level number of identical N and K_a numbers is expected to be two at the most due to the spin splitting. The state mixing must be necessarily considered to account for abnormal level numbers measured.

Figure 3 plots the reduced level energies against $N'(\nu_1)$. The linearity is not apparent in Figure 3 any more. However, one can recognize that each of three groups of $\Delta N' = 0, \pm 1$ consists of one series, which suggests that three vibronic states may contribute to the ν_1-transition from the ground state.

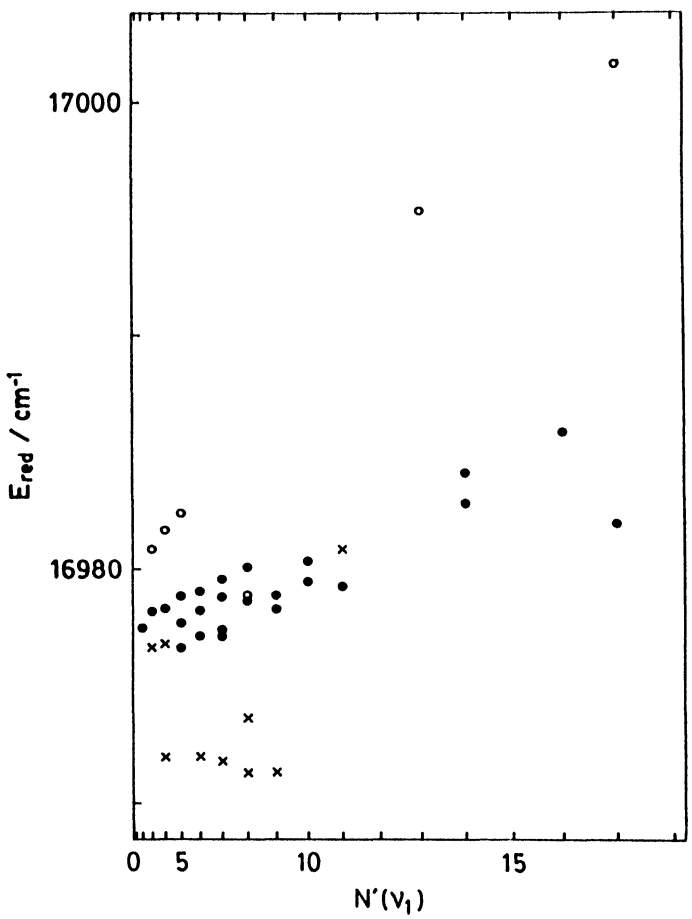

Figure 3 Plot of the reduced rovibronic energies, $E_{red} = E_{evr} - 0.4N'(N' + 1)$, against $N'(N' + 1)$. Here, N′ denotes $N'(\nu_1)$. Three groups of levels may be recognized depending on the interaction selection rules: $\Delta N' = N'(\nu_2) - N'(\nu_1) = +1$ (open circle), 0 (closed circle), and −1 (cross). Fitting of the closed circle data to the equation, $E_{evr} = T_v + (A-\bar{B})K_a^2 + \bar{B}N(N + 1)$, gives the molecular constants; $T_v \sim$ 16,947 cm^{-1} and $\bar{B}$ ~0.41 cm^{-1} assuming that $(A-\bar{B})$ = 7.5 cm^{-1}.

We could not detect a $K'_a = 0$ or 1 stack in this OODR experiment, and therefore we can not determine the exact T_v value of this vibronic level. The band origin (T_v) was estimated to be around 16,947 cm^{-1} from the analysis the $K'_a = 2$ data in Figures 2 and 3 under the assumption that $(A-\overline{B}) = 7.5\ cm^{-1}$. The question here is which zeroth-order vibronic states among A_1, A_2 and B_1, and B_2 make the mixed state in this energy region and are detected by the present OODR method.

4.2. State interaction mechanism and OODR spectroscopy

The main experimental features of the mixed state observed in the 590.1 nm region and the assignments of composite zeroth-order states are summarized as follows.

(I) All the ν_1-transitions originating with $\tilde{X}^2A_1(0,0,0)$ are of a parallel type and therefore the composite state of the mixed state responsible for the ν_1-transition is conclusively $^2B_2$.

(II) From the ν_1-transition in OODR, one can classify thirty nine rovibronic levels belonging to the mixed state into three zeroth-order vibronic levels as seen in Figure 3. Three research groups have carried out the jet-cooled LIF experiments in this energy region[2,4,5] and found a strong vibronic band at 16,946.711 cm^{-1}. We can not compare our $K'_a = 2$ data directly with their jet-cooled LIF data, because the jet-cooled experiments provide only the information on the lowest N levels in the $K_a = 0$ stack. The T_v value of the vibronic state, to which the $K'_a = 2$ levels detected by OODR belong, is estimated to around 16,947 cm^{-1}, which accords with the band origin of 16,946.711 cm^{-1} measured in the supersonic jet. Thus, we conclude that at least one of the composite states responsible for the ν_1-transition is the $^2B_2$ vibronic state which has the band origin at 16,946.711 cm^{-1}.

(III) All the ν_2-transitions terminating on 2^2B_2 are of a perpendicular type and therefore the composite state of the mixed state responsible for the ν_2-transition is $^2B_2$ or $\tilde{C}^2A_2$. If the levels of $K'_a = 0$ or 1 are detected, then we could determine whether the vibronic state responsible for the ν_2-transition is B_2 or A_2.[11–13] For the intermediate state studied in this experiment, we could detect only the $K'_a = 2$ levels and it is rather difficult to determine the vibronic symmetry from the rotational structure. The clue may exist in the value of the band origin, $T_v \sim 16{,}947\ cm^{-1}$. We have already reported the T_v values of $\tilde{C}^2A_2$ to be 16,970 cm^{-1} for (0,1,0),[11] and 17,710 cm^{-1} for (0,2,0) or (1,0,0).[13] The vibronic level detected in this study lies about 20 cm^{-1} below $\tilde{C}^2A_2(0,1,0)$ and 690 cm^{-1} above $\tilde{C}^2A_2(0,0,0)$.[16] It is likely that the vibronic state ($T_v \sim 16{,}947\ cm^{-1}$) responsible for the ν_2-transition is not A_2 but B_2. It might be worthy of note here that the B_2 vibronic levels are much dense (one level every 10 cm^{-1}) than the A_2 levels (one level every 500 cm^{-1}) in this energy region. Thus, a mixed state detected in the 590.1 nm region is concluded to be composed of two $^{ev}B_2$ states: One (B''_2 state) and another (B'_2) states are responsible for the ν_1- and ν_2-transitions, respectively.

(IV) The selection rules between $N'_{Ka,Kc}(\nu_1)$ and $N'_{Ka,Kc}(\nu_2)$ are expressed as $\Delta N' = 0, \pm 1$, and $\Delta K'_a = 0$, which implies that the spin–orbit interaction contributes at

least partly to generation of the mixed state. Furthermore in some of ν_2-scanned spectra, we observed abnormally weak ^PQ branches (for example $^PQ_2(14)$), which suggest that an A_1 vibronic state (one level every 10 cm^{-1}) is also included in the mixed state. The similar spin–orbit (and/or orbital–rotation) coupling between B_2 and A_1 vibronic levels is also recognized in the region of 612–614 nm.[10]

(V) Many levels of identical $N'_{Ka,Kc}(\nu_2)$ quantum numbers were detected in a narrow energy region of a few wavenumbers. For example, six levels were detected as $7_{2,5}(\nu_2)$ in the E_{evr} region of 16,999.53–17,002.45 cm^{-1} (Table I). These levels of an identical rotational quantum number scatter over 3 cm^{-1} but may be recognized as a $K'_a = 2$ stack of one severely-perturbed vibronic state as a whole. Due to the nuclear spin (I = 1), NO_2 has six spin sublevels, but the hyperfine splitting is much smaller than spectral resolution of lasers employed. This particular six-level interaction case can be rationalized by a coupling scheme illustrated in Figure 4. Two composite B_2 vibronic levels are required to make the mixed state. They are denoted as B'_2 and B''_2, which are responsible for the ν_2- and ν_1-transitions, respectively. The spin–orbit and orbital–rotation interactions can not mix the vibronic state with identical symmetry (B_2–B_2 interaction). Therefore, the A_1 vibronic state must be considered into the coupling scheme between B'_2 and B''_2. This indirect coupling via A_1 vibronic states accounts for the level number of $7_{2,5}(\nu_2)$. The spin–orbit interaction combines B_2 and A_1 vibronic states with the selection rules that $\Delta N = 0, \pm 1$ and $\Delta K_a = \pm 1$. The orbital–rotation interaction mixes B_2 and A_1 vibronic states under the selection rules

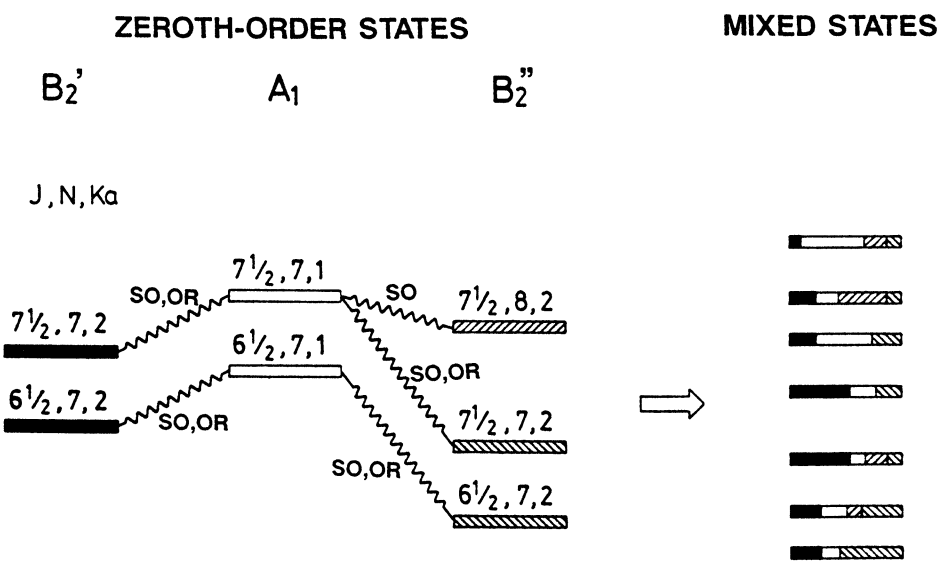

Figure 4 Multi-state coupling scheme for $7_{2,5}(\nu_2)$ levels. The quantum numbers of J, N, and K_a are indicated for the zeroth-order rovibronic levels. The B'_2, A_1, and B''_2 zeroth-order states are shown in the first (filled square levels), second (open square levels), and third (hatched square levels) columns, respectively. Symbols of SO and OR denote spin–orbit and orbital–rotation interactions, respectively. The mixed states are schematically presented in the fourth column. See the text in detail.

that $\Delta N = 0$ and $\Delta K_a = \pm 1$. Hence the A_1 vibronic state with $K_a = 1$ or 3 can interact with the B_2 vibronic state with $K_a = 2$. The experimental results obtained by this OODR study can be reasonably explained by the model described in Figure 4, where the K_a value of the A_1 vibronic state is assumed to be 1.

The complexity of the visible spectrum of NO_2 is caused primarily by the strong vibronic interaction between $\tilde{B}^2B_2$ and $\tilde{X}^2A_1$ states. In addition to vibronic interaction, the spin–orbit and orbital–rotation interactions must be considered to elucidate the interaction network of excited NO_2. In this OODR study we present the experimental evidence to show that A_1 vibronic levels play an important role to perturb the B_2 vibronic levels.

Acknowledgments

The authors are grateful to Professor Kinichi Obi (Tokyo Institute of Technology) for his encouragement throughout of this work and Professor Kentaro Kawaguchi (Nobeyama National Observatory) for his help on the energy calculation.

References

1. D. K. Hsu, D. L. Monts and R. N. Zare. "Spectral Atlas of Nitrogen Dioxide 5530 to 6480 Å" (Academic, New York, 1978); K. Uehara and H. Sasada, "High Resolution Spectral Atlas of Nitrogen Dioxide 559–597 nm" (Springer, Heidelberg, 1985).
2. R. E. Smalley, L. Wharton and D. H. Levy. *J. Chem. Phys.*, **63**, 4977 (1975).
3. S. Hiraoka, K. Shibuya and K. Obi. *J. Mol. Spectrosc.*, **129**, 427 (1987).
4. G. Persch, E. Mehdizadeh, W. Demtröder, Th. Zimmermann, H. Köppel and L. S. Cederbaum. *Ber. Bunsenges. Phys. Chem.*, **92**, 312 (1988).
5. A. Delon, R. Jost and M. Lambardi. *J. Chem. Phys.*, **95**, 5701 (1991).
6. M. Baba, H. Yamada and K. Nishizawa. *J. Chem. Phys.*, **97**, 4569 (1992).
7. J. C. D. Brand and P. H. Chiu. *J. Mol. Spectrosc.*, **75**, 1 (1979).
8. K. Tsukiyama, K. Shibuya, K. Obi and I. Tanaka. *J. Chem. Phys.*, **82**, 1147 (1985).
9. K. Shibuya, T. Kusumoto, H. Nagai and K. Obi. *Chem. Phys. Letters*, **152**, 129 (1988).
10. H. Nagai, K. Shibuya and K. Obi. *J. Chem. Phys.*, **93**, 7656 (1990).
11. H. Nagai, K. Aoki, T. Kusumoto, K. Shibuya and K. Obi. *J. Phys. Chem.*, **95**, 2718 (1991).
12. K. Shibuya, T. Kusumoto, H. Nagai and K. Obi. *J. Chem. Phys.*, **95**, 720 (1991).
13. K. Aoki, H. Nagai, K. Hoshina and K. Shibuya. *J. Phys. Chem.*, (in press)
14. W. C. Bowman and F. C. De Lucia. *J. Chem. Phys.*, **77**, 92 (1982).
15. K.-E. J. Hallin and A. J. Merer. *Can. J. Phys.*, **54**, 1157 (1976).
16 A. Weaver, R. B. Metz, S. E. Bradforth and D. M. Neumark. *J. Chem. Phys.*, **90**, 2070 (1990).